



Contents lists available at ScienceDirect

## Materials Science in Semiconductor Processing

journal homepage: [www.elsevier.com/locate/mssp](http://www.elsevier.com/locate/mssp)

## Current-transport mechanisms in gold/polypyrrole/n-silicon Schottky barrier diodes in the temperature range of 110–360 K

A. Gümüş<sup>a,\*</sup>, Ş. Altındal<sup>b</sup><sup>a</sup> Department of Physics, Faculty of Arts and Sciences, Niğde University, 5100 Niğde, Turkey<sup>b</sup> Department of Physics, Faculty of Sciences, Gazi University, 06500 Ankara, Turkey

## ARTICLE INFO

## Keywords:

Au/PPy/n-Si (MPS) type SBDs  
Current-transport mechanisms  
Temperature dependent  
Barrier inhomogeneity

## ABSTRACT

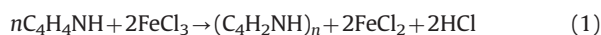
In this study, Au/polypyrrole/n-Si metal-polymer-semiconductor (MPS) Schottky barrier diode (SBD) was fabricated by using a spin coating system for formation of polypyrrole (PPy) organic layer and a thermal evaporation system for deposition of metal contacts. The forward bias current-voltage-temperature ( $I$ - $V$ - $T$ ) characteristics of the diode were investigated in the temperature range of 110–360 K. The some main electrical parameters such as the zero-bias barrier height ( $\Phi_{bo}$ ), ideality factor ( $n$ ), and effective barrier height ( $\Phi_{bef}$ ) were found as function temperature. The experimental results show that the  $I$ - $V$ - $T$  characteristics have a non-linear behavior especially due to the effect of series resistance ( $R_s$ ) and interfacial polymer layer by resulting a higher  $n$  value of 3.09 larger than unity ( $n > 1$ ). While the value of  $\Phi_{bo}$  increases,  $n$  decreases with increasing temperature and such changes in  $\Phi_{bo}$  and  $n$  with temperature was attributed to the presence of saddle point or pinch-off at around mean BH value ( $\bar{\Phi}_{bo}$ ) at M/S interface. The value of Richardson constant ( $A^*$ ) was obtained from the slope of conventional Richardson plot,  $\ln(I_0/T^2)$  vs  $(q/kT)$  as  $1.395 \times 10^{-8} \text{ A/cm}^2 \text{ K}^2$  which is much lower than the known theoretical value of  $112 \text{ A/cm}^2 \text{ K}^2$  for n-Si. The  $\bar{\Phi}_{bo}$  and standard deviation ( $\sigma_0$ ) were obtained from the intercept and slope of  $\Phi_{bo}$  vs  $q/kT$  plot as 1.146 eV and 0.13 V. Thus, the  $\bar{\Phi}_{bo}$  and effective value of  $A^*$  were obtained as 1.078 eV and  $113.03 \text{ A/cm}^2 \text{ K}^2$  from the modified Richardson plot. The obtained experimental value of  $A^*$  is in a good agreement with the theoretical value of  $112 \text{ A/cm}^2 \text{ K}^2$  for n-Si. As a result, current transport mechanism (CTM) in MPS type SBD can be successfully explained on the basis of thermionic emission (TE) theory with Gaussian distribution (GD) of barrier heights (BHs) around  $\bar{\Phi}_{bo}$ .

© 2014 Elsevier Ltd. All rights reserved.

## 1. Theoretical background

Pyrrole can be polymerized electrochemically [1]. Polypyrrole (PPy) is a type of organic polymer formed from polymerization of pyrrole. Polypyrroles are conducting polymers, related members being polythiophene, polyaniline, and polyacetylene [2]. (<http://en.wikipedia.org/wiki/Polypyrrole> - cite\_note-RussChemRev-2) The Nobel Prize in Chemistry was awarded in 2000 for work on conductive

polymers including PPy [3]. Some of the first examples of polypyrroles were reported in 1963 by Weiss and coworkers and they described the pyrolysis of tetraiodopyrrole to produce highly conductive materials [4]. Most commonly Ppy is prepared by oxidation of pyrrole, which can be achieved using ferric chloride in methanol:



Polymerization is thought to occur via the formation of the pi-radical cation  $\text{C}_4\text{H}_4\text{NH}^+$ . This electrophile attacks the C-2 carbon of an unoxidized molecule of pyrrole to

\* Corresponding author.

E-mail address: [agumus38@gmail.com](mailto:agumus38@gmail.com) (A. Gümüş).

give a dimeric radical  $(C_4H_4NH)_2]^+$ . The process repeats itself many times. Conductive forms of PPy are prepared by oxidation ("p-doping") of the polymer:



The polymerization and p-doping can also be affected electrochemically. The resulting conductive polymer is peeled off of the anode.

Films of PPy are yellow but darken in air due to some oxidation. Doped films are blue or black depending on the degree of polymerization and film thickness. They are amorphous, showing only weak diffraction. PPy is described as "quasi-unidimensional" vs one-dimensional since there is some crosslinking and chain hopping. Undoped and doped films are insoluble in solvents but swellable. Doping makes the materials brittle. They are stable in air up to 150 °C at which temperature the dopant starts to evolve (e.g., as HCl) [2].

PPy is an insulator but its oxidized derivatives are good electrical conductors. The conductivity of the material depends on the conditions and reagents used in the oxidation. Conductivities range from 2 to 100 S/cm. Higher conductivities are associated with larger anions, such as tosylate. Doping the polymer requires that the material swell to accommodate the charge-compensating anions. The physical changes associated with this charging and discharging has been discussed as a form of artificial muscle [5]. PPy and related conductive polymers have two main applications in electronic devices and for chemical sensors [6]. PPy is also potential vehicle for drug delivery. The polymer matrix serves as a container for proteins [7]. PPy is also being investigated in low temperature fuel cell technology to increase the catalyst dispersion in the carbon support layers and to sensitize cathode electrocatalysts, as it has been inferred that the metal electrocatalysts (Pt, Co, etc.) when coordinated with the nitrogen in the pyrrole monomers show enhanced oxygen reduction activity [8].

PPy (together with other conjugated polymers such as polyaniline, poly(ethylenedioxythiophene), etc.) has been actively studied as a material for "artificial muscles", a technology that would offer numerous advantages over traditional motor actuating elements [9]. Polypyrrole was used to coat silica and reverse phase silica to yield a material capable of anion exchange and exhibiting hydrophobic interactions [10]. Polypyrrole was used in the microwave fabrication of multiwalled carbon nanotubes, a new method that allows to obtain CNTs in a matter of seconds [11]. Chemical and Engineering News reported in June 2013 that Chinese research has produced a water-resistant polyurethane sponge coated with a thin layer of PPy that absorbs 20 times its weight in oil and is reusable [12].

A metal-semiconductor (MS) junction forms the Schottky barrier diodes (SBDs) whose properties depend on the metal's work function, the band gap of the intrinsic semiconductor, the type and concentration of dopants in the semiconductor, and other factors. Additionally, the presence of a thin interfacial insulator or polymer layer between metal and semiconductor, which is named as metal-insulator/polymer-semiconductor (MIS/MPS), is also known as SBDs.

However, lately, MPS structures become more popular compared to MIS structures due to their industrial applications. Especially, organic semiconductors used in electronic and photonic devices have many advantages compared to inorganic semiconductors, such as easy fabrication, low cost and large-area applications on both rigid and flexible substrates. All these advantages makes the organic semiconductors very attractive for use as active components for organic light emitting diodes (OLEDs), transistors as well as organic lasers, organic field effect transistors (OFETs), organic photodiodes (OPDs), solar cells and other solid state electronic devices like Schottky diodes. Heterojunction and SBDs fabricated and tested by using different semiconducting organic and inorganic compounds have gained considerable importance on characteristics of electronic devices. The electrical and dielectric properties of electronic devices strongly depend on the interface states and polymeric interfacial layer in MPS structures. It is believed that the use of high dielectric interfacial insulator or polymer layer can considerably reduce the leakage current, the amount of surface states and series resistance. In addition, it is not only isolated from metal to semiconductor but also obstacle the inter-diffusion between metal and semiconductor. Therefore, in recent years, some researchers started the use of an interfacial polymer layer with high dielectric constant instead of conventional SiO<sub>2</sub> and they observed a significant improvement in the diode performance [17–19]. Therefore, organic materials as charge transfer (CT) compounds are attractive since they are promising materials for developing organic based electronic devices applications.

The enhancement of MPS device performance by organic interfacial layer in SBDs was studied by inserting new organic materials, such as polyvinyl alcohol, perylene, rhodamine-101, chitin, etc., at metal-semiconductor (M/S) interface. In addition to enhancement in device performance, improvement in rectification behavior of diode can be achieved by using organic interfacial layer instead of inorganic interfacial layer. To improve the device performance of MPS Schottky barrier diodes, understanding the control mechanisms of electrical characteristics is quite important. The density of interface states ( $N_{ss}$ ) at metal/polymer (M/P) or polymer/semiconductor (P/S) interface, series resistance ( $R_s$ ) of MPS diodes and the barrier height at metal/semiconductor (M/S) interface can be deduced from current-voltage ( $I$ - $V$ ) analysis and affect the performance of MPS diodes.

In this study,  $I$ - $V$  measurements were performed in dark and in the temperature range of 110–360 K for Au/PPy/n-Si (MPS) Schottky barrier diode. The essential electrical parameters such as ideality factor ( $n$ ), zero-bias barrier height ( $\Phi_{bo}$  or  $\Phi_{bef}$ ),  $R_s$  and shunt resistance ( $R_{sh}$ ) and  $N_{ss}$  were obtained from the temperature dependent  $I$ - $V$  measurements. Experimental results show that all parameters were found as a strong function of temperature. The observed anomaly decrease in  $n$  and increase of  $\Phi_{bo}$  with increasing temperature were explained by single Gaussian distribution of BH.

## 2. Experimental details

The Au/PPy/n-Si SBDs were fabricated on n-type (phosphor doped) float zone (100) single crystal Si wafer. Firstly,

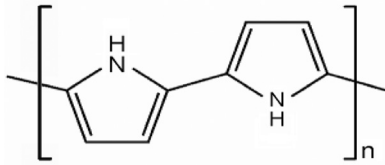


Fig. 1. Chemical structures of PPy.

the wafer was cleaned with RCA cleaning procedure. High purity Au metal (5 N) with a thickness of  $\sim 1500$  Å was thermally evaporated onto the whole back side of Si wafer in a pressure about  $10^{-6}$  Torr in a high vacuum thermal evaporation system. In order to perform good ohmic behavior, Si wafer was annealed at  $450$  °C in pressure of  $10^{-6}$  Torr. The PPy film was deposited on n-type Si substrate by thermal evaporation technique and its chemical structures are given in Fig. 1. After deposition of PPy thin film, circular dots of 1 mm diameter and  $1500$  Å thick high purity (5 N) Au rectifying contacts were formed on the PPy surface of the wafer through a metal shadow mask in high vacuum system at about  $10^{-6}$  Torr. In this way, Au/PPy/n-Si SBDs were fabricated for the electrical measurements and the electrode connections were made by silver paste. The thickness of interfacial PPy layer ( $d$ ) was obtained from the interfacial layer capacitance  $C_i (= \epsilon' \epsilon_0 A/d)$  as  $55$  Å at  $1$  MHz.

Current–Voltage ( $I$ – $V$ ) measurements were performed by means of a Keithley 2400 source-meter in the wide temperature range of  $110$ – $360$  K using a temperature controlled Janis VPF-475 cryostat with vacuum of  $\sim 10^{-3}$  Torr. The sample temperature was always monitored by using a copper-constantan thermocouple close to the sample, and measured with a Keithley 2400 source-meter and with the help of Lake Shore model 321 auto-tuning temperature controllers with sensitivity better than  $\pm 0.1$  K. All measurements were carried out with the help of a microcomputer through an IEEE-488 ac/dc converter card.

### 3. Results and discussion

An overview of forward and reverse bias  $I$ – $V$  characteristics of Au/PPy/n-Si (MPS) SBD in the temperature range of  $110$ – $360$  K is shown on a semi-logarithmic scale in Fig. 2. The difference in the work functions of the electrodes implying different barriers at metal/polymer (M/P) interface gives rise to the asymmetrical nature of the curve which denotes the excellent rectification characteristic of diode. The existence of an interfacial polymer layer and  $N_{ss}$  leads to a high ideality factor ( $n > 1$ ). Usually the semi-logarithmic forward bias  $I$ – $V$  plots deviated from the linearity due to the effect of  $R$  at enough high forward biases. By considering these effects, the  $I$ – $V$  characteristic of Au/PPy/n-Si (MPS) SBD, according to thermionic emission (TE), can be expressed by the following relation:

$$I = I_0 \left[ \exp \left( \frac{q(V - IR_s)}{nkT} - 1 \right) \right] \quad (3)$$

where  $V$  is the applied bias voltage, the term  $IR_s$  is the voltage drop across  $R_s$ ,  $n$  is the ideality factor,  $k$  is the

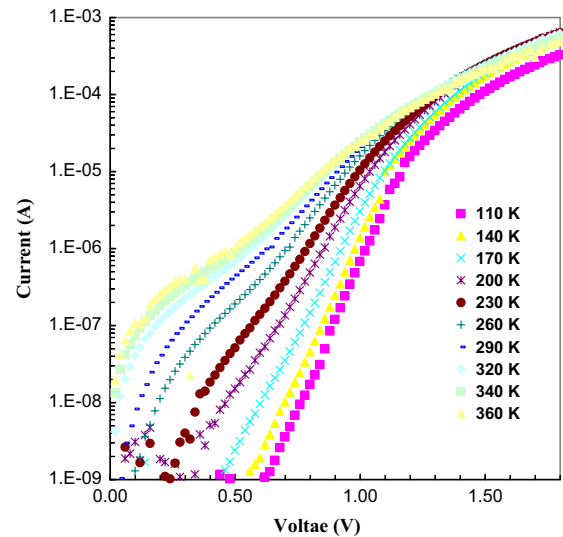


Fig. 2. Semi-logarithmic  $I$ – $V$  characteristics of Au/PPy/n-Si (MPS) SBD in the forward bias region in the temperature range of  $110$ – $360$  K.

Boltzmann constant,  $T$  is the absolute temperature in Kelvin,  $q$  is the electronic charge and  $I_0$  is the reverse saturation current derived from the straight line intercept of  $\ln I$ – $V$  plot at zero bias, and is given by [13–16].

$$I_0 = AA^* T^2 \exp \left( -\frac{q\Phi_{bo}}{kT} \right) \quad (4)$$

where  $A$ ,  $A^*$ ,  $\Phi_{bo}$  are the rectifier contact area, effective Richardson constant (equal to  $112$  A/cm $^2$  K $^2$  for n-type Si [17,18]), and the zero-bias barrier height, respectively. The ideality factor measures the deviation of practical diodes from ideal thermionic emission theory and determines the slope of the exponential regime of the dark  $I$ – $V$  characteristics on a semi-logarithmic plot through the following relation [13]:

$$n = \frac{q}{kT} \frac{d(V - IR_s)}{d(\ln I)} \quad (5)$$

The value of  $\Phi_{bo}$  can be extracted from Eq. 2 (extrapolated  $I_0$ ) and it can be written as follows:

$$\Phi_{bo} = \frac{kT}{q} \ln \left( \frac{AA^* T^2}{I_0} \right) \quad (6)$$

The semi-logarithmic  $I$ – $V$  curve of the device in dark in the temperature range of  $110$ – $360$  K is shown in Fig. 2 which gives information about the rectifying behavior of the diode, the leakage current, the interface states, the series and the shunt resistance of the device. There is a linear relationship for low applied voltages while there is a deviation from linearity at high applied voltage values, which may be a result of the voltage drop across the series resistance in the natural region of the semiconductor. The obtained main Schottky barrier diode parameters such as  $n$ ,  $I_0$ ,  $\Phi_{bo}$  and  $\Phi_{eff}$  values are given in Table 1.

As can be seen in Table 1,  $I_0$ ,  $\Phi_{bo}$  and  $n$  values range from  $3.92 \times 10^{-14}$ ,  $0.282$  eV,  $6.48$  (at  $110$  K)  $4.32 \times 10^{-8}$ ,  $0.841$  eV,  $3.77$  (at  $360$  K), respectively. It is clear that the value of  $\Phi_{bo}$  increases and  $n$  decreases with increasing

**Table 1**

The obtained main Au/PPy/n-Si (MPS) SBD parameters for various temperatures.

T (K)	$I_0$ (A)	$n$	$\Phi_{bo}$ (eV)	$\Phi_{bef}$ (eV)
110	$3.92 \times 10^{-14}$	6.48	0.287	1.132
140	$1.82 \times 10^{-13}$	5.31	0.489	1.133
170	$2.44 \times 10^{-12}$	5.10	0.561	1.157
200	$4.16 \times 10^{-11}$	4.98	0.617	1.112
230	$2.94 \times 10^{-10}$	4.89	0.676	1.094
260	$2.20 \times 10^{-9}$	4.74	0.725	1.011
290	$6.72 \times 10^{-9}$	4.30	0.786	0.927
320	$1.82 \times 10^{-8}$	4.01	0.845	0.865
340	$3.20 \times 10^{-8}$	3.91	0.885	0.845
360	$4.32 \times 10^{-8}$	3.77	0.931	0.841

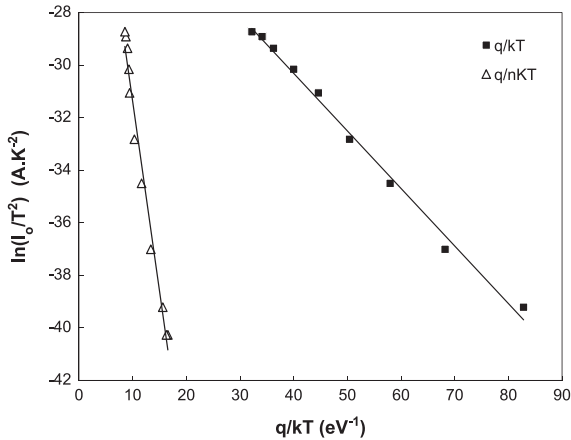


**Fig. 3.** Richardson plot of  $\ln(I_0/T^2)$  vs  $1/T$  for the Au/PPy/n-Si Schottky diode according to the Gaussian distributions of barrier heights.

temperature. This change in  $\Phi_{bo}$  and  $n$  with temperature can be attributed to the presence of saddle point or pinch-off in the depletion region. The calculated value of  $n$  for each temperature is higher than unity ( $n > 1$ ) that indicates the deviation from ideality and shows the non-ideal  $I$ - $V$  behavior in the semiconductor devices. This can be attributed to the existence of interfacial polymer layer, high density of  $N_{ss}$  localized at metal/polymer (M/P) interface, high value of  $R_s$ , the effect of barrier inhomogeneities and tunneling effect [14,19–25]. It is believed that the barrier height value of Au/PPy/n-Si (MPS) SBD maybe improved the performance of the diode compared with the conventional Au/n-Si diode [16,17]. The PPy organic blend which modifies the interfacial electrical parameters of Au/n-Si diodes and the effective barrier height by affecting the space charge region of the n-Si can be the result of this increase in  $\Phi_{bo}$ . The high value of  $n$  and low value of barrier height especially at low temperature are a result of the barrier in-homogeneity at M/S interface rather than interfacial layer.

As can be seen from Fig. 3, the decrease in BH at low temperatures leads to the nonlinearity in the activation energy plot ( $\ln(I_0/T^2)$  vs  $q/kT$ ). However, the ( $\ln(I_0/T^2)$  vs  $q/nkT$ ) plot gives a straight line (Fig. 3). Such non-linearity activation energy plot is caused by the temperature dependence of the BH and  $n$ . The origin of the decrease

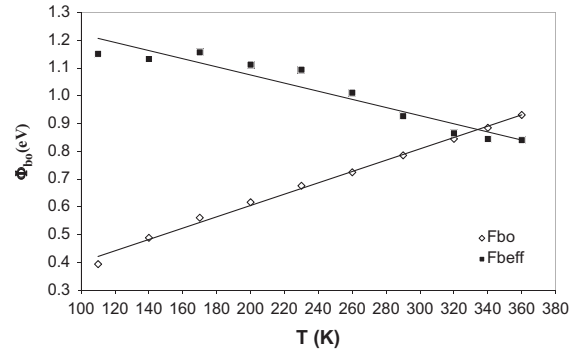


**Fig. 4.** Temperature dependence of the ideality factor and barrier height for the Au/PPy/n-Si Schottky contact.

in the BH and increase in ideality factor with decrease in temperature in the SBDs may be attributed to the presence of Schottky barrier height (SBH) inhomogeneity [26–30]. SBH inhomogeneities can be explained by assuming specific distribution of nanometer. The temperature dependent  $\Phi_{bo}$  and  $\Phi_{ef}$  vs  $T$  plots are given in Fig. 4. The value of Richardson constant  $A^*$  was obtained from the intercept of  $\ln(I_0/T^2)$  vs  $q/kT$  and  $q/nkT$  as  $1.95 \times 10^{-8}$  A/cm<sup>2</sup> K<sup>2</sup> and  $2.636 \times 10^{-7}$  A/cm<sup>2</sup> K<sup>2</sup>, respectively, and these values are  $8.03 \times 10^9$  and  $4.25 \times 10^8$  times lower than the theoretical value of  $A^*$  (112 A/cm<sup>2</sup> K<sup>2</sup>). The  $E_a$  values were also obtained from the slope of these plots and these values are  $8.03 \times 10^9$  and  $4.25 \times 10^8$  times lower than the theoretical value of  $A^*$  (112 A/cm<sup>2</sup> K<sup>2</sup>). The  $E_a$  values were also obtained from the slope of these plots

The  $E_a$  value of 1.435 eV is higher than the value of forbidden band gap of Si. In order to obtain the modified BH values ( $\Phi_{bef}$ ), both the  $\ln(I_0/T^2)$  vs  $q/kT$  and  $\ln(I_0/T^2)$  vs  $q/nkT$  plots were drawn (Fig. 3). The linearity of  $\ln(I_0/T^2)$  vs  $q/nkT$  plot confirmed that the expression of  $I_0$  should be included  $n$  and tunneling parameter ( $-\alpha\chi^{0.5}\delta$ ) values and it can be described as [31]

$$I_0 = AA^*T^2 \exp(-\alpha\chi^{0.5}\delta) \exp\left(-\frac{q\Phi_{bef}}{kT}\right) \quad (7)$$

where  $\Phi_{bef}$  is the effective BH and  $\alpha$  is a constant that depends on tunneling effective mass of electrons ( $m_e^*$ ). The value of electron tunneling factor ( $\alpha\chi^{0.5}\delta$ ) was obtained from the Richardson plot as 22.8. Thus, the  $\Phi_{bef}$  values were obtained from Eq. 5 for each temperature and are tabulated in Table 1. As shown in Fig. 4, while the value of  $\Phi_{bo}$  increases  $\Phi_{ef}$  decreases with increasing temperature and have  $-15 \times 10^{-4}$  eV negative temperature coefficient. Thus the negative temperature coefficient of BH is closer to the negative temperature coefficient of the forbidden bandgap of Si ( $-4.3 \times 10^{-4}$  eV K<sup>-1</sup>).

Assuming a GD of the BHs, the relation between  $\Phi_{bo}$  and temperature can be written as follows [27–30]:

$$\Phi_{bo} = \bar{\Phi}_{bo}(T=0) \frac{q\sigma_0^2}{2kT} \quad (8)$$

where  $\bar{\Phi}_{bo}$  and  $\sigma_0$  are the Gaussian parameters of the BH distribution and the temperature dependence of  $\sigma_0$  is usually small and can be neglected. In addition, the



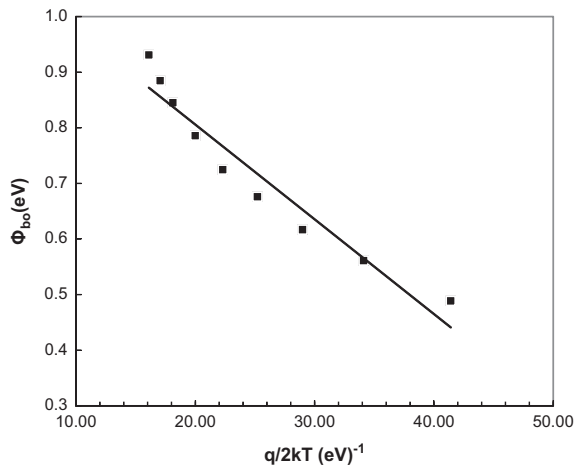


Fig. 5. Barrier height vs  $1/2kT$  curves of the Au/PPy/n-Si Schottky diodes according to the Gaussian distributions of the barrier height.

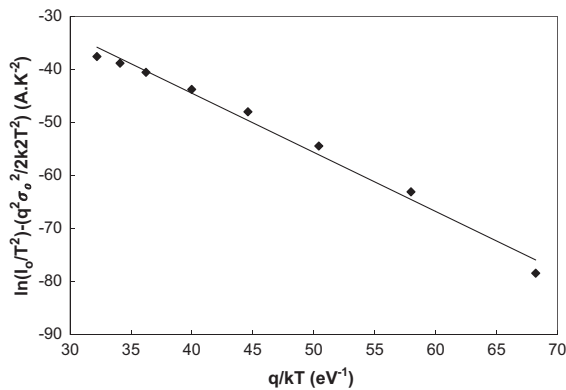


Fig. 6. The modified Richardson plot of  $\ln(I_0/T^2) - (q^2\sigma_0^2/2k^2T^2)$  vs  $q/kT$  for Au/PPy/n-Si SBD.

variation of  $n$  with temperature in GD model is given by [24–27].

$$\left(\frac{1}{n} - 1\right) = \rho_2 - \frac{q\rho_3}{2kT} \quad (9)$$

Therefore,  $\Phi_{bo}$  vs  $q/2kT$  plot was drawn to obtain evidence of a Gaussian distribution (GD) of the BHs and it is given in Fig. 5. As can be seen in Fig. 5, the  $\Phi_{bo}$  vs  $q/2kT$  plot shows a linear behavior and the mean values of  $\bar{\Phi}_{bo}$  and standard deviation ( $\sigma_0$ ) were obtained from the intercept and slope of this plot as 1.146 eV and 0.13 V. Thus, the conventional Richardson plot was modified by combining Eqs.(2) and (6) as [27–31] and given in Fig. 6.

$$\ln\left(\frac{I_0}{T^2}\right) - \left(\frac{q^2\sigma_0^2}{2k^2T^2}\right) = \ln(AA^*) - \frac{\bar{\Phi}_{bo}}{kT} \quad (10)$$

As can be seen from Fig. 6, the modified  $\ln(I_0/T^2) - (q^2\sigma_0^2/2k^2T^2)$  vs  $q/kT$  plot has also a straight line. The value of  $\bar{\Phi}_{bo}$  was obtained as 1.078 eV from the slope of this plot and the value of  $A^{**}$  was obtained as 113.03 A/cm<sup>2</sup> K<sup>2</sup> its intercept ( $=AA^{**}$ ) by using rectifier contact area. This experimental value of  $A^*$  ( $=113.03$  A/cm<sup>2</sup> K<sup>2</sup>) obtained

from the modified Richardson plot is in a good agreement with the theoretical value of 112 A/cm<sup>2</sup> K<sup>2</sup> for n-Si. The obtained experimental result, current-transport mechanism in Au/PPy/n-Si (MPS) type SBD can be successfully explained on the basis of TE theory with GD of BHs around mean BH ( $\bar{\Phi}_{bo}$ ).

#### 4. Conclusion

Metal–polymer–semiconductor (Au/PPy/n-Si) type Schottky barrier diode (SBD) was fabricated using spin coating system. The PPy film was deposited on an n-type Si substrate by thermal evaporation technique. The forward bias  $I$ – $V$ – $T$  characteristics of the diode have been investigated in the temperature range of 110–360 K. The values of electrical parameters such as  $I_0$ ,  $\Phi_{bo}$  and  $n$  were found as a function of temperature and were found as a strong function of temperature with their values ranging from  $3.92 \times 10^{-14}$ , 0.282 eV, 6.48 (at 110 K)  $4.32 \times 10^{-8}$ , 0.841 eV, 3.77 (at 360 K), respectively.  $I$ – $V$ – $T$  characteristics show a non-linear behavior due to the effect of series resistance  $R_s$ , resulting in a higher ideality factor value of 3.09 larger than unity ( $n > 1$ ). The obtained results confirmed that the main parameters of Au/PPy/n-Si MPS SBD were mainly affected by the PPy interfacial organic layer and  $R_s$ . While the value of  $\Phi_{bo}$  increases,  $n$  decreases with increasing temperature. Such changes in  $\Phi_{bo}$  and  $n$  with temperature was attributed to the presence of pinch-off or patches at around mean value of  $\bar{\Phi}_{bo}$  at M/S interface. The slope of conventional Richardson plot,  $\ln(I_0/T^2)$  vs  $(q/kT)$  has given the Richardson constant ( $A^*$ ) of  $1.395 \times 10^{-8}$  A/cm<sup>2</sup> K<sup>2</sup> which is much lower than the theoretical value of 112 A/cm<sup>2</sup> K<sup>2</sup> for n-Si. The  $\bar{\Phi}_{bo}$  and  $\sigma_s$  values were obtained from the intercept and slope of  $\Phi_{bo}$  vs  $q/kT$  plot as 1.146 eV and 0.13 V, respectively. Thus,  $\bar{\Phi}_{bo}$  and  $A^*$  were obtained as 1.078 eV and 113.03 A/cm<sup>2</sup> K<sup>2</sup> from the modified Richardson plot, respectively. This value of  $A^*$  ( $=113.03$  A/cm<sup>2</sup> K<sup>2</sup>) is in a good agreement with the theoretical value of 112 A/cm<sup>2</sup> K<sup>2</sup> for n-Si. Experimental results confirmed that the CTM in Au/PPy/n-Si (MPS) type SBD can be successfully explained on the basis of TE theory with GD of BHs around  $\bar{\Phi}_{bo}$ .

#### References

- [1] Trans IChemE, Part B, Process Safety and Environmental Protection, 85 (2007) 489.
- [2] V.V. Tat'yana, O.N. Efimov, Russ. Chem. Rev. 66 (1997) 443.
- [3] A.G. MacDiarmid, Angew. Chem. Int. Ed. 40 (2001) 2581.
- [4] R. McNeill, R. Siudak, J.H. Wardlaw, D.E. Weiss, Aust. J. Chem. 16 (1963) 1056.
- [5] R.H. Baughman, Science 308 (2005) 63.
- [6] J. Jiri, M. Josowicz, Nat. Mater. 21 (2003) 19.
- [7] S. Geetha, R.K. Rao Chepuri, M. Vijayan, D.C. Trivedi, Anal. Chim. Acta 568 (2006) 119.
- [8] M.U. Sreekuttan, M.D. Vishal, K.P. Vijayamohan, S. Kurungot, J. Phys. Chem. C 114 (2010) 14654.
- [9] T.S. Olson, S. Pylypenko, P. Atanassov, K. Asazawa, K. Yamada, H. Tanaka, J. Phys. Chem. C 114 (2010) 5049.
- [10] <http://atmsp.whut.edu.cn/resource/pdf/4987.pdf>.
- [11] <http://www.sciencedirect.com/science/article/pii/S002196739185003X>.
- [12] <http://www.pubs.rsc.org/en/content/articlelanding/2011/CC/C1CC13359D>.

- [13] S.M. Sze, *Physics of Semiconductor Devices*, second ed. Wiley, New York, 1981.
- [14] E.H. Rhoderick, R.H. Williams, *Metal–Semiconductor Contacts*, Clarendon Press, Oxford, 1988.
- [15] H.C. Card, E.H. Rhoderick, *J. Phys. D* 4 (1971) 1589.
- [16] M. Gökçen, T. Tunç, Ş. Altındal, İ. Uslu, *Curr. Appl. Phys.* 12 (2012) 525.
- [17] S. Demirezen, Z. Sönmez, U. Aydemir, Ş. Altındal, *Curr. Appl. Phys.* 12 (2012) 266.
- [18] M. Abkowitz, J.S. Facci, J. Rehm, *J. Appl. Phys.* 83 (1998) 2670.
- [19] K. Akkılıç, M.E. Aydın, İ. Uzun, T. Kılıçoğlu, *Synth. Metals* 156 (2006) 958.
- [20] S.K. Cheung, N.W. Cheung, *Appl. Phys. Lett.* 49 (1986) 85.
- [21] H.C. Card, E.H. Rhoderick, *J. Phys. D* 4 (1971) 1589.
- [22] Z. Çaldıran, A.R. Deniz, Ş. Aydoğan, A. Yesildag, D. Ekin, *Superlattices Microstruct.* 04 (2013) 45.
- [23] Y.P. Song, R.L. Van Meirhaeghe, W.H. Laflere, F. Cardon, *Solid State Electron.* 29 (1986) 6633.
- [24] R.F. Schmitsdorf, T.U. Kampen, W. Mönch, *Surf. Sci.* 324 (1995) 249.
- [25] J.H. Werner, H.H. Güttler, *J. Appl. Phys.* 69 (1991) 1522.
- [26] Z.J. Horvath, *J. Appl. Phys.* 64 (1988) 6780.
- [27] Ş. Karataş, Ş. Altındal, A. Türüt, A. Özmen, *Appl. Surf. Sci.* 217 (2003) 250.
- [28] R.F. Schmitsdorf, T.U. Kampen, W. Mönch, *Surf. Sci.* 324 (1995) 249.
- [29] W. Mönch, *J. Vac. Sci. Technol. B* 17 (1999) 1867.
- [30] H.H. Güttler, J.H. Werner, *Appl. Phys. Lett.* 56 (1990) 1113.
- [31] A. Gümüş, A. Türüt, N. Yalçın, *J. Appl. Phys.* 91 (2002) 91.